PET Imaging of Osteosarcoma*

Winfried Brenner, MD, PhD[1]; Karl H. Bohuslavizki, MD, PhD[2]; and Janet F. Eary, MD[1]

[1]*Division of Nuclear Medicine, University of Washington Medical Center, Seattle, Washington; and* [2]*Department of Nuclear Medicine, University Hospital Eppendorf, Hamburg, Germany*

During the past decade the clinical value of PET imaging has been investigated for many different tumors. As knowledge of the advantages and limitations of this modality increased, PET has gained acceptance in tumor imaging. ^{18}F-FDG PET is now successfully used and approved for procedure reimbursement in many types of cancer—for example, lung cancer, melanoma, lymphoma, head and neck tumors, brain tumors, esophageal cancer, and colorectal cancer. In osteosarcoma, the introduction of neoadjuvant chemotherapy has dramatically improved survival rates, thus changing the demands for state-of-the-art imaging to provide detailed information on tumor staging and grading, evaluating treatment, and detecting recurrences. In this review, the available literature on PET imaging in osteosarcoma patients is critically summarized with respect to diagnosis, staging, therapy monitoring, and follow-up focusing on the clinically used tracers ^{18}F-FDG and ^{18}F-fluoride ion. Potential and probable indications are outlined. Because of the relatively small number of patients enrolled in clinical trials published to date, further research needs to be done in larger, prospective patient series to determine the full utility of PET in osteosarcoma.

Key Words: osteosarcoma; ^{18}F-FDG; ^{18}F-fluoride ion; PET; metabolic imaging

J Nucl Med 2003; 44:930–942

Despite the fact that osteosarcoma represents only 0.1% of all tumors, it is the second most frequent malignant primary bone tumor after myeloma. The incidence has no sex- or race-based predilection and is estimated to be about 2 or 3 per 10^6 persons. More than 80% of all cases present in patients between 5 and 25 y of age. A second lower peak incidence occurs in the fifth and sixth decades (*1*). Etiologically, osteosarcoma can be divided into 2 categories: primary and secondary types. Primary osteosarcoma predominantly affects the metaphyseal portion of the long bones of the extremities, with approximately 30% of cases occurring in other skeletal locations (*1*). The fundamental nature of osteosarcoma is yet unknown. In contrast, secondary osteosarcoma often arises in locations of Paget's disease, fibrous dysplasia, and multiple chondromas or is associated with retinoblastoma. It is also observed after radiation therapy, with most of the cases developing within 7–15 y after irradiation. Outcome is usually poor in secondary osteosarcoma as compared with primary osteosarcoma, and the majority of these tumors is located in the truncus, craniofacial, or even extraskeletal (*1*).

CLASSIFICATION AND STANDARD DIAGNOSTIC PROCEDURES

According to the clinical staging criteria of the Union Internationale Contre le Cancer (UICC) in 1997, osteosarcoma patients are divided into 6 groups based on the TNM stage and histologic grading (Tables 1 and 2) (*2*). Although osteosarcoma is a heterogeneous disease with a large range of pathologic presentations (Table 3), at the time of primary diagnosis as many as 75% of all patients are classified as clinical stage IIB. This presentation consists of a histologic grade 3 or 4 with tumor extension to the periosteum without evidence of lymph node and distant metastases (Fig. 1) (*1*,*3*). However, in 80% of these patients occult metastases must be presumed on the basis of the experience in the prechemotherapy era that these patients will develop metastases within months, which are predominantly located in the lungs (Fig. 2). Moreover, osteosarcoma frequently metastasizes to second bone sites, which occurs in 10%–20% of patients with metastatic disease, whereas lymph node involvement is rarely seen. The prognosis of osteosarcoma was poor before the development of effective chemotherapy, with 80% of the patients dying within 2 y (*4*). Introduction of multiagent chemotherapy has improved survival rates, reaching 60%–70% in recent years (*4*,*5*).

Because the therapeutic management of osteosarcoma as well as treatment of recurrent disease has been significantly improved with aggressive chemotherapeutic regimens, accurate tumor staging and restaging after treatment have become increasingly important in osteosarcoma patients. The pretherapeutic diagnostic work-up usually starts with conventional radiography of the tumor-suspicious bone and subsequent biopsy. The diagnosis of osteosarcoma is then based on characteristic histologic features in combination with typical radiographic findings. MRI of the entire sus-

Received Aug. 29, 2002; revision accepted Dec. 11, 2002.

For correspondence or reprints contact: Winfried Brenner, MD, PhD, Division of Nuclear Medicine, University of Washington Medical Center, 1959 N.E. Pacific St., P.O. Box 356113, Seattle, WA 98195-6113.

E-mail: winbren_2000@yahoo.com

*NOTE: FOR CE CREDIT, YOU CAN ACCESS THIS ACTIVITY THROUGH THE SNM WEB SITE (http://www.snm.org/education/ce_online.html) THROUGH JUNE 2004.

TABLE 1
Histologic Tumor Grading of Osteosarcoma

Tumor grade	Tumor differentiation
G1	Well differentiated
G2	Moderately differentiated
G3	Poorly differentiated
G4	Undifferentiated
Gx	Not assessable

pected bone is performed to define the degree of penetration of the tumor surrounding soft tissue as well as to estimate the local tumor infiltration into bone marrow (*6–9*). Arteriography has been used for presurgical treatment planning to assess possible vascular involvement (*10*) but is usually replaced by MRI and color-coded duplex sonography nowadays. Furthermore, CT of the chest and conventional bone scanning are necessary (*5,11*) because metastases of osteosarcoma are known for their early hematogenous spread with predilection for the lungs and the skeleton. Posttreatment follow-up imaging consists of radiography or CT of the chest in 6-mo intervals. This is especially important because the treatment of lung metastases is still potentially curative by complete surgical resection of lung nodules. MRI and bone scanning are used to distinguish postoperative changes from residual or recurrent tumor tissue after local surgical treatment. Because osteosarcoma metastases usually incorporate bisphosphonates, bone scanning can be used for follow-up examinations to detect both osseous and nonosseous metastases.

TREATMENT AND OUTCOME

According to the Cooperative Osteosarcoma Study Group, the standardized therapeutic management of osteosarcoma includes neoadjuvant chemotherapy followed by wide resection of the primary tumor, which is still considered the only reliable step to ensure local tumor control (*4,12*). Today, limb-sparing procedures are most often performed rather than amputations in patients with tumors of the limbs (*13–15*). However, as compared with ablative surgical procedures, limb-sparing surgery itself has a 3- to 5-fold increased risk of local relapse, which significantly worsens prognosis (*16,17*). According to the data of the Cooperative Osteosarcoma Study Group (*3,18*), the overall survival rate after 5 y is 68%, whereas prognosis of patients with a local relapse deteriorates dramatically with a survival rate after 5 y of only 21%. Therefore, effective multidrug pre- and postoperative chemotherapy is mandatory to reduce the risk of local relapse. Preoperative, neoadjuvant chemotherapy, however, also provides an important prognostic factor in osteosarcoma because a greater degree of drug-induced tumor necrosis is associated with a significantly higher survival rate (*12,18*). Necrosis of ≥90% of the tumor mass is considered as a good therapy response. Moreover, chemotherapy treats potential metastatic spread. After adjuvant chemotherapy, fewer lung metastases have been observed and the metastases appear later than in the prechemotherapy era. Combined treatment protocols increased disease-free and overall survival rates after 5 y in patients with no detectable metastases initially from 20% in the case of surgery only to 60%–70% with the use of neoadjuvant chemotherapy (*3,4*). Because osteosarcoma is relatively resistant to radiation therapy, this treatment modality is used mainly in inoperable tumors or when a complete surgical resection cannot be achieved, as may be the case in tumors of the spine. Patients with tumor relapse usually have lung metastases only. As long as these metastases are completely resectable by surgical metastasectomy, there is still a 20%–

TABLE 2
Clinical Staging of Osteosarcoma Based on Tumor Grade and TNM

Tumor grade	TNM	Clinical stage
G1, G2	T1 N0 M0	IA
G1, G2	T2 N0 M0	IB
G3, G4	T1 N0 M0	IIA
G3, G4	T2 N0 M0	IIB
Any G	Any T, N1 M0	IVA
Any G	Any T, any N, M1	IVB

Stage III is not defined.

TABLE 3
Classification of Osteosarcoma

Classification	%
Primary high-grade, intramedullary	75
Mixed pattern (73%)	
Bone rich/sclerosing (9%)	
Cartilage rich (5%)	
Spindle cell rich	
Malignant histiocyte rich	
Telangiectatic	
Small cell rich (Ewing-like)	
Benign giant cell rich	
Epitheloid cell rich	
Primary low-grade, intramedullary	4–5
Fibrous dysplasia-like (50%)	
Nonossifying fibroma-like (25%)	
Osteoblastoma-like (15%)	
Chondromyxoid fibroma-like (10%)	
Secondary intramedullary	6
Multifocal	1–2
Intracortical	0.2
Juxtacortical	7–10
Parosteal (65%)	
Periosteal (25%)	
High-grade surface (10%)	
Osteosarcoma of jaw	6

Classification according to Mirra (*1*).

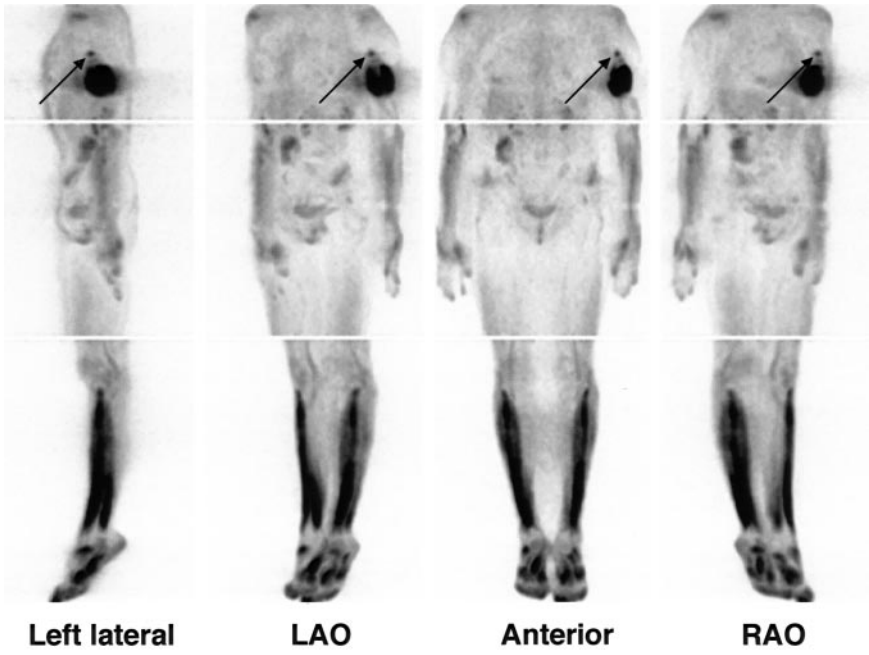

FIGURE 1. Maximum intensity projections of truncus and extremities of patient with primary high-grade mixed pattern osteosarcoma of left humerus. Intense tracer accumulation of ^{18}F-FDG is evident at primary tumor site with second focus of less uptake (arrow) above, suggesting a skip metastasis. LAO = left anterior oblique; RAO = right anterior oblique.

50% chance of cure in selected cases (*19*). Therefore, early detection of small lung metastases is one of the most challenging and critical tasks in the follow-up of osteosarcoma patients.

PET

Because both the management and the outcome of osteosarcoma have been improved by the introduction of reliable staging systems (Table 4) as a basis for adequate therapy (*20*,*21*), sophisticated diagnostic procedures are important to ensure accurate tumor staging and restaging. Therefore, apart from conventional, well-standardized anatomic imaging procedures, metabolic PET imaging became the focus of ongoing research by assessing its potential utility in sarcoma patients (*22*)—for example, for determining the metabolic rates of osteosarcoma (*23*–*28*), monitoring of neoadjuvant therapy response (*29*–*32*), and differentiating viable sarcoma from posttreatment changes (*33*–*36*). The most widely used PET tracer for osteosarcoma is ^{18}F-FDG. The other clinical PET tracer with reported utility for osteosarcoma imaging in patients is ^{18}F-fluoride ion (^{18}F), whereas ^{18}F-labeled monoclonal antibodies (*37*), ^{18}F-fluoromi-

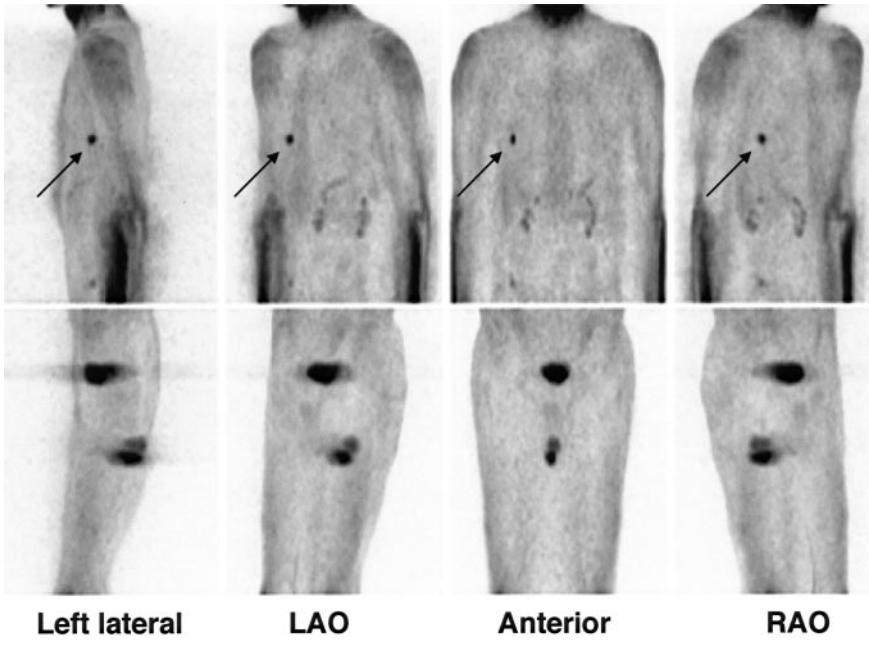

FIGURE 2. Maximum intensity projections of truncus of patient after therapy of osteosarcoma of right tibia and newly diagnosed small lung mass detected by conventional radiography in follow-up study. Focal accumulation of ^{18}F-FDG in right apical lobe (arrow) confirms viable tumor tissue. LAO = left anterior oblique; RAO = right anterior oblique.

TABLE 4
Surgical Staging System by Enneking et al. (*20*)

Tumor grade	Tumor site	Stage
Low	Intracompartmental*	IA
Low	Extracompartmental†	IB
High	Intracompartmental	IIA
High	Extracompartmental	IIB
Low or high	Metastasis (regional or distant)	III

*Intramedullary without breaching cortex.
†Tumor extends beyond cortex.
Only 2 tumor grades are used, either high or low.

sonidazole (*38*), ^{18}F-labeled RGD-containing glycopeptide (*39,40*), ^{3}H-thymidine (*38*), ^{13}N-methionine (*41*), and PET of p53 transcriptional activity in osteosarcoma (*42*) have been used only in animal studies.

^{18}F-FDG

Physiology

^{18}F-FDG is the most widely used PET tracer in oncology and the most commonly used tracer for osteosarcoma imaging (Figs. 3, 4, and 5). ^{18}F-FDG PET studies produce images that represent the rate of glycolysis in tissues: The glucose analog 2-^{18}F-FDG undergoes membrane transport and phosphorylation by hexokinase to ^{18}F-FDG-6-phosphate similar to the pathway of glucose metabolism to glucose-6-phosphate. However, whereas glucose-6-phosphate is metabolized in the normal glycolysis pathway, ^{18}F-FDG-6-phosphate is not a substrate for further metabolism. Because ^{18}F-FDG is not able to diffuse back across the cell membrane after phosphorylation nor can phosphorylation be reversed to a significant extent, ^{18}F-FDG is trapped in the cell in proportion to the rate of glycolysis. This metabolic pathway enables ^{18}F-FDG to be used for quantitative metabolic imaging. Common quantitative procedures for ^{18}F-FDG imaging in tumor (*27*) are the standard uptake value (SUV) (*43*), graphical analysis (*44–46*), and nonlinear regression analysis based on a 3-compartment model for ^{18}F-FDG (*47*). The tumor SUV is a semiquantitative parameter that represents the metabolic activity in a static image as measured by region-of-interest (ROI) technique and corrected for both the injected activity per kilogram of body weight and the blood glucose level. Two different types of SUV are known that represent different biologic information. The average tumor SUV is the mean of all pixel-related SUV values within an ROI as a statistical measure of tumor metabolism in general. However, in heterogeneous tumors such as osteosarcoma, the maximum SUV—that is, the highest single SUV value within an ROI—is thought to be more reliable to describe biologic features because the highest uptake areas determine tumor grade. Patlak analysis and the more sophisticated nonlinear regression analysis allow true quantitative calculation of kinetic parameters but re-

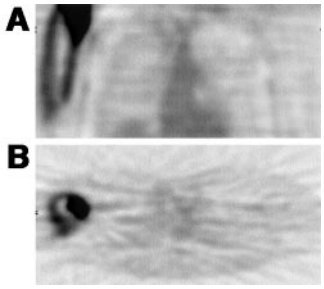

FIGURE 4. Coronal (A) and transverse (B) projections of primary high-grade, mixed-pattern osteosarcoma in right proximal humerus. Pretherapeutic maximum SUV was 16.2 in this large and inhomogeneous tumor with low ^{18}F-FDG uptake in tumor center. According to high SUV, overall survival in patient was poor.

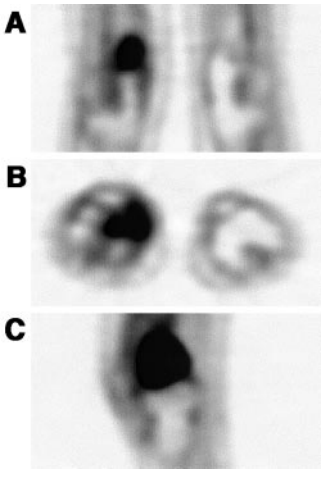

FIGURE 3. Coronal (A), transverse (B), and sagittal (C) projections of telangiectatic high-grade osteosarcoma in right distal femur. Initial ^{18}F-FDG SUV was 6.5 in this rather homogeneous tumor.

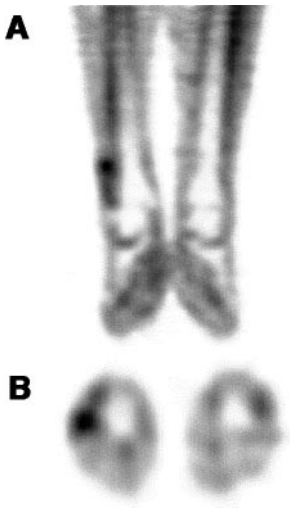

FIGURE 5. Coronal (A) and transverse (B) projections of small periosteal osteosarcoma in right distal fibula reveal initial ^{18}F-FDG SUV of 1.6.

quire dynamic PET in combination with arterial or venous blood sampling.

First Imaging Studies

Because glycolysis is enhanced in most malignancies, inflammatory lesions, and some benign tumors, ^{18}F-FDG has been widely used for tumor imaging. In the 1980s, when ^{18}F-FDG PET studies began to focus on oncology, a report was published on the usefulness of ^{18}F-FDG in osteosarcoma imaging. In 1988, Kern et al. (*22*) successfully imaged 4 patients with soft-tissue tumors and 1 patient with an osteogenic tumor using ^{18}F-FDG PET. Although the number of patients was very small in this study, the highest ^{18}F-FDG uptake values were found in high-grade tumors. Similar findings were reported by Adler et al. in 1991 (*23*) for 25 patients with musculoskeletal tumors including 2 patients with osteosarcoma. In grade 3 tumors, ^{18}F-FDG uptake was significantly higher than in grade 1 tumors or benign lesions, demonstrating a positive correlation ($r = 0.83$) of tumor grade and ^{18}F-FDG uptake. In 1993, Hoh et al. (*48*) successfully detected tumor lesions with intense ^{18}F-FDG uptake in 3 of 4 osteosarcoma patients. In 1 patient with recurrent disease at the resected primary site, the ^{18}F-FDG study was negative. That lesion, however, consisted of almost entirely necrotic tissue and contained only microscopic foci of tumor.

Thus, these early PET studies already demonstrated the feasibility of detecting osteosarcoma with ^{18}F-FDG and laid the basis for further investigations. Osteosarcomas generally showed intense ^{18}F-FDG uptake. Semiquantitative findings suggested a correlation of tumor ^{18}F-FDG uptake and histologic grading, whereas normal bone was characterized by relatively low ^{18}F-FDG uptake. Subsequent studies describing tumor ^{18}F-FDG PET in osteosarcoma patients investigated the impact of this imaging modality on tumor grading, staging (i.e., diagnosis of tumor presence and extension as well as metastatic spread), therapy monitoring, and detection of recurrences during follow-up.

Osteosarcoma Tumor Grading

Many publications on the use of ^{18}F-FDG PET in osteosarcoma patients describe tumor uptake as a measure of metabolic activity and, thus, of tumor grade. Early studies by Kern et al. (*22*) and Adler et al. (*23*) reported higher uptake values in high-grade tumors. In short, all of the published papers show a correlation of histologic grading or tumor aggressiveness with ^{18}F-FDG uptake, measured as tumor-to-background ratio (TBR), SUV, or kinetic modeling analysis results. However, at present, the published ^{18}F-FDG imaging results do not suggest avoiding tumor biopsy to differentiate benign from malignant lesions because of overlaps in ^{18}F-FDG uptake in both processes. To our knowledge, only 1 publication so far has shown no correlation between the metabolic rate of glucose consumption and the biologic aggressiveness, making it impossible to differentiate between benign and malignant bone tumors (*49*). Both the SUV and the Patlak-derived metabolic rate of FDG (MR_{FDG}) showed a wide overlap between 19 malignant and 7 benign bone tumors (the mean maximum SUV in malignant tumors ranged from 2.93 to 16.06 vs. 2.23–12.27 in benign tumors). However, in this study by Kole et al. (*49*) 2 observations are quite interesting: First, osteosarcomas with low MR_{FDG} responded poorly to subsequent chemotherapy, whereas 1 patient with a high MR_{FDG} responded well; and, second, osteosarcomas revealed relatively low MR_{FDG} as compared with malignant fibrous histiocytoma or lymphoma.

This is in contrast to the findings of Eary et al. (*26*), who reported that osteosarcomas displayed the highest MR_{FDG} values beside the malignant fibrous histiocytoma. Thus, the relatively low MR_{FDG} values, at least in the case of osteosarcoma, might be an explanation for the poor correlation between tumor uptake and grading observed by Kole et al. (*49*). Also, in contrast to the findings of Kole et al., Griffeth et al. (*50*) could correctly separate 10 malignant from 10 benign lesions of soft-tissue masses by measuring tumor uptake ratios. In line with these findings, Dehdashti et al. (*51*) were able to define intraosseous lesions in 25 patients as either benign or malignant in all cases but one using a cutoff SUV value of 2.0.

Several papers on tumor grading of bone and soft-tissue sarcomas by means of quantitative ^{18}F-FDG PET were published by Eary et al. (*24*,*26*), Eary and Mankoff (*52*), and Folpe et al. (*53*). Despite a high correlation of the SUV and the Patlak-derived metabolic rate of ^{18}F-FDG with a correlation coefficient of 0.94 in 42 soft-tissue and bony sarcomas (*52*), MR_{FDG} was more sensitive for determining tumor grade in a subsequent study (*26*). Although an overlap between the different groups of histologic grade was found with a wide range of variability in MR_{FDG} within any one group, the mean MR_{FDG} values for the different groups were significantly different in 70 patients with bone (13 osteosarcomas) or soft-tissue sarcoma. Highly metabolically active tumors with a low histologic grade may be the reason for the clinical experience that there is a subset of tumors in which the histologic grade does not predict outcome. In a recent paper, Eary et al. (*24*) proved the baseline maximum tumor SUV as an independent and significant predictor of overall survival by means of multivariate analysis in 209 patients with different types and grades of sarcoma (52 patients with osteogenic sarcoma). The *P* values for the baseline maximum SUV were even lower than for histologic tumor grades, showing a higher significance of baseline SUV for prediction of outcome as compared with conventional tumor grading. The authors, therefore, suggest performance of quantitative ^{18}F-FDG PET because of its additional clinical information (Fig. 4).

Another important result is that often a marked heterogeneity of ^{18}F-FDG tumor uptake was observed, with areas of high metabolic activity often in the peripheral tumor parts (*26*). This information on tumor biology, provided by no other radiologic imaging modality, may be important to guide biopsy, because the highest grade areas determine the

histologic tumor grade and predict outcome. The accuracy of tumor diagnosis and histologic grading may suffer from sampling error, particularly in large, heterogeneous tumors (Fig. 6). Non-PET–guided biopsy might miss the most biologically significant region, resulting in a false low pretherapeutic tumor grading. In another study of the Eary group, Folpe et al. (*53*) investigated the relationship of ^{18}F-FDG PET values and pathologic features in 89 patients with soft-tissue tumors or osteosarcoma: They found a significant positive correlation between the tumor SUV and the histopathologic grade, tumor cellularity, Ki-67 labeling and mitotic activity, and overexpression of p53. Because these parameters, either independent or nonindependent predictors of outcome, are associated with higher tumor grade, shortened overall survival, and development of distant metastases, the results suggest a significant role for quantitative ^{18}F-FDG PET in the management of sarcoma patients in terms of reliably separating low-grade tumors that are usually treated by surgery from intermediate or high-grade sarcoma that undergo preoperative neoadjuvant chemotherapy. The ^{18}F-FDG tumor uptake values can be used as pathologic surrogates obtained noninvasively. However, Folpe et al. (*53*) pointed out some limitations of ^{18}F-FDG PET. Because of the wide overlap of SUV values, although the mean group values are significantly different, PET is not able to distinguish between grade II and III tumors. Furthermore, some benign highly cellular and proliferative tumors, such as giant cell tumor of bone, have higher SUV values than grade I sarcomas. Their conclusion, therefore, is that PET scans will not obviate the need for biopsy and tissue diagnosis in soft-tissue and bone masses, whereas PET is helpful to guide biopsy.

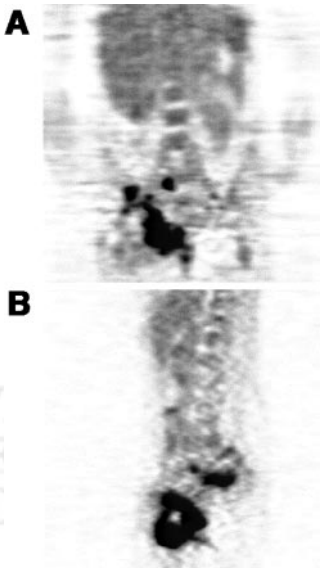

FIGURE 6. Coronal (A) and sagittal (B) projections of large primary high-grade chondroblastic osteosarcoma in right pelvis. Maximum SUV in tumor with heterogeneous ^{18}F-FDG uptake was 7.4.

Similar results stressing the heterogeneity of tumor uptake reflecting different tumor activity areas and necrosis are reported by Lodge et al. (*27*), who studied the kinetics of ^{18}F-FDG tumor uptake over time using the SUV, Patlak analysis, and nonlinear regression analysis to measure ^{18}F-FDG tumor concentrations in benign and malignant soft-tissue masses. The most important result of this study is the difference in time–activity curves between high-grade sarcomas, reaching the peak tumor activity as late as 4 h after ^{18}F-FDG injection, and benign and low-grade tumors, with a peak activity within the first 30 min after injection. The SUV measured at 4 h after injection was as useful as MR_{FDG}, reaching a sensitivity of 100% and a specificity of 76% for the detection of high-grade sarcomas, whereas neither quantitative approach was able to distinguish low-grade sarcomas from benign lesions, as already shown by other authors (*23*,*52*,*53*). In a line with the findings of Lodge et al., Schulte et al. (*54*) reported on 202 patients with bone lesions, 44 of them with osteosarcoma, in whom a cutoff level of 3.0 of the TBR yielded a sensitivity of 93% and a specificity of 67% to detect malignancies. Again, the authors were not able to clearly differentiate aggressive benign lesions from low-grade malignant bone tumors. Using a similar study setting, Aoki et al. (*55*) also observed a significant difference in the mean SUV between malignant and a wide variety of benign bone disorders in 52 patients. Although osteosarcomas presented relatively high SUV values, giant cell tumors, fibrous dysplasia, sarcoidosis, and Langerhans cell histiocytosis reached the same high SUV levels. Thus, a cutoff level of SUV could not be set to safely distinguish between these benign lesions and osteosarcoma. As mentioned by the authors, a possible explanation for the high SUV values observed in these benign lesions is the composition of many of these lesions of either monocyte/macrophage–derived cells or fibroblasts, which are known to have high levels of ^{18}F-FDG metabolism. This finding is also true for inflammatory lesions. As a consequence of high ^{18}F-FDG uptake levels in inflammation, Watanabe et al. (*56*) found high SUV values in sites of osteomyelitis. The imaging studies showed a sensitivity of 100% and a specificity of 77% for ^{18}F-FDG PET in diagnosing malignant bone lesions with an accuracy of 83% using an SUV cutoff of 1.9. However, osteomyelitis and malignant bone tumors could not be differentiated. Interestingly, in 18 bone lesions, the highest SUV values—even higher than in osteosarcoma—were observed in bone metastases.

Osteosarcoma Staging and Restaging

Although ^{18}F-FDG PET showed a very high sensitivity in detecting primary osteosarcoma lesions (*49*,*54*,*57*), it is not considered a diagnostic tool to prove the presence of osteosarcoma. ^{18}F-FDG PET, however, is gaining importance for initial characterization of biologic features of osteosarcoma in terms of tumor grading and treatment planning. Plain radiographs and MRI are the first-line diagnostic tools (*10*). MRI is the technique of choice for defining the intra- and

extraosseous extent of a bone tumor (*58*). Only in children, there might be an indication for ^{18}F-FDG PET to detect intraosseous skip metastases (*59*) in cases of unequivocal MRI findings due to the physiologic red blood marrow distribution in the long bones in children, which may impair the detection of bone metastases (*10,60*). These small lesions can be missed by conventional bone scanning (*61*). However, up to now, no data are available to support this hypothesis as the basis for recommending ^{18}F-FDG PET for that indication.

Because lymph node metastases are very rare in osteosarcoma (*1*), the value of imaging modalities capable of detecting lymph node involvement is rather limited.

Clinical experience showed that in 80% of the patients with no detectable metastases at the time of diagnosis, occult metastases must be presumed, which are predominantly located in the lungs. Early detection of lung metastases, therefore, is important to improve survival because there is a real chance of cure by surgical metastasectomy. Today, the method of choice for detection of lung metastases is spiral high-resolution CT and, because of this technique, the number of lung metastases detected during initial staging has almost doubled (*4*). Nevertheless, many of these presumed metastases have sizes in the submillimeter range and are not detectable. Another common problem is the differentiation of a single or few lung lesions as benign versus metastasis by CT, especially when lesions are relatively small. Schulte et al. (*30*) reported on lung metastases detection in 4 of 27 osteosarcoma patients with no false-positive or false-negative findings according to the CT data. These results suggest a 100% sensitivity and specificity for ^{18}F-FDG PET compared with CT but no superiority of PET with regard to lung metastases. Similar findings were described by Lucas et al. (*36*) in soft-tissue sarcomas. However, in this study, ^{18}F-FDG PET as a whole-body imaging device was able to detect 13 other sites of metastases not shown by CT or MRI because of the limited body area of scanning. Franzius et al. (*62*) compared the results of 32 osteosarcoma patients with a total of 49 ^{18}F-FDG PET scans with spiral CT: The sensitivity, specificity, and accuracy of ^{18}F-FDG PET for lung metastases was 50%, 100%, and 92%, respectively; for CT the corresponding results were 75%, 100%, and 96%. The conclusion of this study was that the sensitivity of ^{18}F-FDG PET for lung metastases was unsatisfactory, especially in small lesions of $<$9 mm. However, similar to previous findings, 15 additional lesions (bone and soft-tissue metastases) were found by PET, which were not detected by conventional staging. These findings were confirmed by a more recent paper from this group (*63*).

Osteosarcoma frequently metastasizes to secondary bone sites in 10%–20% of patients with metastatic disease. Data on the benefit of ^{18}F-FDG PET for detecting osseous metastases in osteosarcoma patients, however, are very sparse with only few patients being imaged so far. Franzius et al. presented successful detection of all sites (n = 6) of bone involvement in a recent publication (*63*). This is in contradiction to their earlier study reporting that none of 5 metastases identified by bone scanning in osteosarcoma could be identified by ^{18}F-FDG PET (*64*). In another study from this group that compared bone scanning, MRI, and ^{18}F-FDG PET in children with primary bone tumors, there was only 1 case presenting a single bone metastasis from osteosarcoma. This lesion showed no ^{18}F-FDG uptake (*65*). Despite reports on increased sensitivity and specificity of ^{18}F-FDG PET for detecting bone metastases in various cancers and soft-tissue sarcomas compared with conventional bone scanning, ^{18}F-FDG PET cannot be recommended for identification of bone metastases in osteosarcoma patients on the basis of the data provided so far.

For osteosarcoma metastases located outside the lungs and bones, no systematic data that compare ^{18}F-FDG PET with other imaging modalities are available. Only a few cases have been reported (*36,62,63*). That might be due to the fact that such metastases can be only detected by CT or MRI when they are located in the scanning field of interest. In contrast to this limitation of CT and MRI, whole-body imaging is considered the great advantage of ^{18}F-FDG PET by several authors (*30,36,62*).

Therapy Monitoring

Response to preoperative neoadjuvant chemotherapy is the most important prognostic factor in osteosarcoma because the degree of drug-induced tumor necrosis is highly correlated with disease-free survival after therapy (*12,18*). Thus, a method that is capable of reliably predicting early tumor response would be of great benefit both for assessing therapeutic outcome and for minimizing ineffective chemotherapy with all of its side effects. Because biochemical changes in tumor are thought to occur earlier in response to treatment than morphologic changes, functional imaging has high clinical utility (Fig. 7). Radiologic methods that describe morphologic changes have been shown to be of limited value for prediction of chemotherapy response (*66*). In 2000, Messa et al. (*58*) stated that ^{18}F-FDG PET is the method of choice for therapy monitoring among all of the available nuclear medicine procedures in their commentary on musculoskeletal neoplasms. In the few studies published so far (*29,30,32,65,67,68*), a positive correlation of FDG uptake and viable tumor tissue has been shown, suggesting ^{18}F-FDG PET as a tool for assessing the efficacy of neoadjuvant chemotherapy. Jones et al. (*29*) investigated the impact of ^{18}F-FDG PET in treatment monitoring of soft-tissue and musculoskeletal sarcoma in 9 patients, 3 of them with high-grade osteosarcoma. They observed a 25%–50% reduction of the peak and average SUV 1–3 wk after initiation of neoadjuvant chemotherapy in tumors with $>$90% necrosis and concluded that ^{18}F-FDG PET would be useful in this clinical setting. However, ^{18}F-FDG uptake was also observed in immature granulation tissue and a fibrous pseudocapsule of a treated tumor, indicating that posttherapeutic tumor uptake represents not only viable tumor tissue but also benign, reactive tissue, resulting in a potential

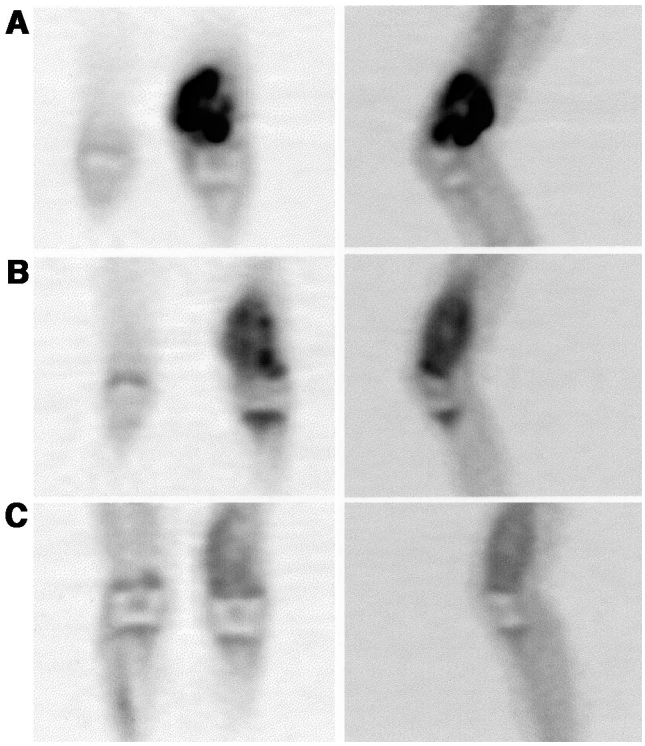

FIGURE 7. Therapy monitoring in patient with primary high-grade, mixed-pattern osteosarcoma of left femur. Initial prechemotherapy SUV (A) was 10.8 in this large and heterogeneous tumor. ^{18}F-FDG PET before third cycle of chemotherapy showed decreased SUV of 4.1 (B), which dropped further to 1.5 at end of chemotherapy before surgical resection (C). According to large drop in SUV, good tumor response was found with <5% viable cells.

overestimation of the remainder of the osteosarcoma. A good correlation between the decrease in posttherapeutic TBRs and the histologic extent of tumor necrosis was also reported by Schulte et al. (*30*) in 27 patients with osteosarcoma undergoing neoadjuvant chemotherapy. A reduction in TBR of >40% detected responders with an accuracy of 92.6%, although the extent of TBR reduction did not precisely predict the quantitative amount of tumor necrosis. No false-positive results were obtained—that is, classifying a histologically proven responder as a nonresponder because of elevated TBR due to inflammatory processes. Nair et al. (*67*) confirmed the value of serial ^{18}F-FDG PET for predicting the percentage of tumor necrosis induced by neoadjuvant chemotherapy in a study of 16 osteosarcoma patients. However, similar to the findings of Schulte et al. (*30*), the percentage change of serial TBR failed to predict a 90% or higher rate of tumor necrosis. However, visual assessment and TBR values of the presurgical, postchemotherapy scans were accurate in 15 of 16 patients. Contrary to these findings, Franzius et al. (*32*) reported a good correlation between tumor necrosis and ^{18}F-FDG uptake measured as a percent reduction of tumor-to-nontumor ratios in 11 patients with osteosarcoma. Using a threshold of a 30% decrease in this ratio, good responders (<10% viable tumor cells) could be distinguished from poor responders in all cases. However, the value of this study is limited by the small number of only 2 persons with poor response. Hawkins et al. (*68*) demonstrated a significant correlation between the drop in SUV and tumor necrosis but found an even more accurate association of low postchemotherapy SUV and good histologic response in 18 osteosarcoma patients. However, both parameters were imperfect at clearly distinguishing a good response (>90% necrosis) from an unfavorable response in 16% and in 27% of the patients using postchemotherapy SUV and the drop in SUV, respectively. One reason for this may be increased ^{18}F-FDG metabolism caused by inflammatory infiltrates or reactive fibrosis within the responding tumor. Another possible explanation is also discussed by the authors. The histopathologic evaluation averages the percentage of tumor necrosis across the entire resected tumor specimen, whereas maximum SUV values within the tumors were used for this study, representing the most active tumor tissue regardless of the size. Thus, the drop in the average SUV of the whole tumor might be more useful than the maximum SUV to predict the amount of necrosis. However, to predict outcome, the maximum SUV is thought to be more precise in delineating areas of insufficient therapy response.

Although the number of patients is still relatively small, ^{18}F-FDG PET seems to reliably predict tumor response in neoadjuvant chemotherapy (*69*). This would be of particular interest because CT and MRI do not always reflect the quantity of residual viable tumor. Gadolinium enhancement is also present in immature scar tissue and nonmalignant reactive tissue (*10*,*70*,*71*). Although a new dynamic contrast-enhanced MRI technique has been shown to improve differentiation of viable osteosarcoma tissue from tumor necrosis and to early identify patients at risk of recurrence (*72*–*74*), the clinical benefit of this method has yet to be proven.

Local Tumor Recurrences

Besides the detection of newly developed metastases summarized above in the Staging and Restaging section, differentiation of fibrosis and posttherapeutic tissue changes due to healing from residual tumor tissue or local relapse is the most challenging task in the follow-up of osteosarcoma patients (Fig. 8). Reviewing the role of nuclear medicine in primary bone and soft-tissue tumors, Abdel-Dayem (*69*) considered ^{18}F-FDG PET to be more accurate than CT or MRI in the follow-up of treated bone and soft-tissue sarcoma patients for differentiating fibrosis from recurrence. Most of the papers supporting this statement, however, describe imaging results relating to soft-tissue tumors. Garcia et al. (*33*) found ^{18}F-FDG PET helpful in differentiating active musculoskeletal sarcomas from posttreatment changes as confirmed by histology or long-term follow-up in 48 patients including 18 patients with osteosarcoma, yielding an overall sensitivity and specificity of 98% and 90%, respectively. el-Zeftawy et al. (*75*) reported similar

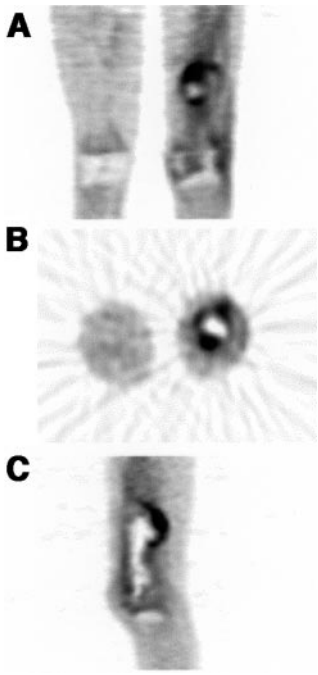

FIGURE 8. Coronal (A), transverse (B), and sagittal (C) projections of locally relapsing osteosarcoma in left distal femur 7 mo after primary surgery. Area of pronounced ^{18}F-FDG uptake (SUV, 3.4) is evident at proximal end of resection site, which was histologically confirmed as tumor recurrence.

findings in 20 patients with bone and soft-tissue tumors. They concluded that ^{18}F-FDG PET, besides CT and MRI, proved to have additional impact on the clinical management of these patients in helping to differentiate postoperative change from local recurrence. Moreover, detection of all local recurrences in 6 osteosarcoma patients has been reported by Franzius et al. (*63*). ^{18}F-FDG was false-positive only in 1 case. In the same patient group, MRI also detected all 6 recurrences but revealed 2 false-positive results. In a study by Lucas et al. (*36*), comparing MRI and ^{18}F-FDG PET, on detection of local recurrences after amputation in patients with sarcomas, MRI had a higher sensitivity of 88.2% compared with 73.7% for PET. However, in osteosarcoma, MRI is often hampered by imaging artifacts after implantation of a metallic prosthesis (*10*). In these patients, ^{18}F-FDG PET is expected to be superior to MRI for detection of local recurrences. Furthermore, Lucas et al. found 13 other sites of metastases by ^{18}F-FDG PET, suggesting that CT of the chest, MRI of the tumor region, and whole-body ^{18}F-FDG PET are necessary to define accurately the extent of disease.

Conclusions and Future Perspectives of ^{18}F-FDG

In studies reviewed above, it is not yet possible to draw definite indications for ^{18}F-FDG PET in osteosarcoma because the number of studies and the number of enrolled patients are too small. Furthermore, the methods used for the different studies—for example, time of PET study before or after intervention, imaging procedure, and method of quantification—differ per study. Because osteosarcoma is a rare tumor, multicenter trials using well-defined diagnostic and therapeutic settings seem to be the appropriate tool to increase the data on ^{18}F-FDG PET for the various considerable indications suggested so far.

Primary Staging. For the basic work-up of bone lesions, plain radiographs and MRI are the first-line diagnostic tools for description and definition of extent of a bone tumor. High-resolution CT has been shown to be superior to ^{18}F-FDG PET for detecting lung metastases, and ^{18}F-FDG PET also cannot be recommended for the search of bone metastases in osteosarcoma patients on the basis of the data provided so far. It seems more promising to evaluate the clinical benefit of ^{18}F PET bone imaging for the latter purpose. For primary staging, ^{18}F-FDG PET has reduced utility. The exception may be in children, where there may be an indication for ^{18}F-FDG PET, or ^{18}F PET, to detect intraosseous skip metastases in cases of unequivocal MRI findings, although no data are yet available to support this hypothesis.

Tumor Grading and Prognosis. Because an overlap of ^{18}F-FDG uptake values between different tumor grades is reported, it is usually not possible to differentiate low-grade and sometimes high-grade osteosarcoma from ^{18}F-FDG–avid benign lesions, such as giant cell tumors or osteomyelitis. Thus, the results do not permit avoiding biopsy. ^{18}F-FDG PET, however, is helpful for targeting biopsy in large, heterogeneous tumors to achieve a representative tumor specimen because the highest-grade areas determine the histologic grade and subsequent biologic behavior. This information on tumor biology cannot be provided by other radiologic imaging devices. Another interesting topic that should be further evaluated in clinical studies is highly metabolically active but histologically low-grade tumors. In a subset of tumors the histologic grade does not predict outcome. Furthermore, initial high ^{18}F-FDG uptake is predictive of poor overall and event-free survival. Clinical follow-up studies in these patients will clarify whether ^{18}F-FDG PET is more accurate for prediction of outcome than conventional clinical tumor grading.

Therapy Monitoring. ^{18}F-FDG PET imaging data show reliability for prediction of tumor response to preoperative, neoadjuvant chemotherapy. This is of particular interest because CT and MRI images do not always detect the quantity of residual viable tumor. Further ^{18}F-FDG PET studies on larger patient populations are necessary to confirm recent promising findings and to define the most suitable parameter to predict the amount of tumor necrosis—that is, the percentage change of uptake or, simply, the posttherapeutic ^{18}F-FDG uptake value. The influence of inflammatory or healing processes on postchemotherapy tumor uptake also has to be determined by correlating histologic findings with imaging results. Future studies need to define how early after the onset of chemotherapy is ^{18}F-FDG PET able to precisely predict tumor response. This definition would allow minimization of ineffective treat-

ment and support an earlier change to alternative chemotherapeutic regimens or even to surgery in case of unsuccessful chemotherapy. For an individualized risk evaluation to further improve therapy, new PET tracers might be helpful—for example, ^{11}C-verapamil. Because the majority of relapsing patients revealed Pgp-positive primary tumors, it would be helpful to know the status of MDR1-induced chemotherapy resistance (*76–78*). Other PET tracers for further characterization of biologic features might be ^{18}F-misonidazole to define hypoxia, which influences angiogenesis, proliferation, and glucose metabolism within the tumor, or ^{11}C-thymidine to provide data on tumor DNA synthesis and cell proliferation.

Patient Follow-Up. For differentiation between benign residual mass lesions caused by posttherapeutic tissue changes and residual tumor tissue or local relapse, ^{18}F-FDG PET is considered to be highly sensitive and more accurate than CT or MRI. In the case of osteosarcoma, MRI is often hampered by image artifacts after implantation of metallic prostheses. As stated for primary staging, there is no clear indication for ^{18}F-FDG PET for detection of lung or bone metastases. However, ^{18}F-FDG PET was able to detect distant metastases in addition to CT and MRI because metastases can be detected by these imaging modalities only when they are located within the scanning field of interest. In contrast to this limitation of CT and MRI, whole-body imaging is considered the great advantage of ^{18}F-FDG PET by many authors. They suggest that CT of the chest, MRI of the tumor region, and whole-body ^{18}F-FDG PET are necessary to accurately define the extent of disease. This significantly influences further therapy choices because it is known that patients with metastatic spread benefit from both surgery and second-line chemotherapy (*4*).

In conclusion, there are clinical settings in which ^{18}F-FDG PET is already helpful for patient management in osteosarcoma:

- Predicting outcome as well as tumor response in neoadjuvant chemotherapy
- Differentiating postoperative changes from residual tumor tissue or local relapse
- Whole-body imaging for detecting hematogenous spread during follow-up; in the case of diagnosed lung masses, PET is helpful to differentiate benign from metastatic lesions.

^{18}F

^{18}F is a well-known bone-seeking tracer used for bone imaging for 4 decades. However, there are only a few publications on ^{18}F bone PET and even fewer on the use of ^{18}F PET in patients with osteosarcoma.

Physiology

^{18}F is extracted from plasma in proportion to bone perfusion (*79–82*) following a clearly defined physiologic process that allows quantitative studies of the skeletal system using dynamic PET procedures (*82*). Hawkins et al. (*83*) suggested a 3-compartment, 4-parameter kinetic model for ^{18}F behavior consisting of the plasma space and an unbound and a bound bone compartment. Fluoride is taken up by the bones from the plasma into the unbound bone compartment and then undergoes ionic exchange with hydroxyl groups in hydroxyapatite to form fluoroapatite (bound fraction). Fluoride does not diffuse into mature bone but is incorporated during bone mineralization (*84*). The rate constants for these processes (k_1 and k_2 for the forward and reverse capillary transport to the unbound bone compartment, k_3 for binding to bone apatite, and k_4 for the release from fluoroapatite) can be measured by dynamic PET in combination with arterial or venous blood sampling over 60–90 min after injection of ^{18}F by using standard nonlinear regression methods. According to this compartment model, the forward macroparameter ^{18}F bone influx rate $K_i = k_1 \times k_3/(k_2 + k_3)$ can be calculated as a measure of bone metabolism (*83,85–88*). The influx rate can also be estimated by Patlak graphical analysis in good correlation with the modeling results (*83,88*). Unfortunately, no quantitative ^{18}F bone PET studies on osteosarcoma for diagnostic purpose or for therapy monitoring have been published so far.

Imaging Studies

The positron emitter ^{18}F was introduced for bone scanning using conventional gamma-camera systems by Blau et al. in 1962 (*89*). ^{18}F was then approved by the Food and Drug Administration for clinical use and became the standard agent for bone scanning until the development of ^{99m}Tc-labeled bisphosphonates in the 1970s. A first report on the use of ^{18}F for skeletal PET in cancer patients was published by Hoh et al. in 1993 (*90*). Among 13 patients with documented malignant bone lesions, 4 had osteosarcoma. The 3 highest tumor-to-normal bone activity ratios of all the patients investigated were observed in untreated osteosarcoma as compared with other malignant bone lesions. In a patient with proven lung metastases of osteogenic sarcoma, Hoh et al. also found an increased ^{18}F uptake in these metastases. Interestingly, in 1 patient with osteosarcoma after treatment with chemo- and immunotherapy, the tumor activity ratio was clearly reduced to about one third of those observed in untreated osteosarcoma, suggesting quantitative PET with ^{18}F as a useful tool for monitoring therapy response. The only other clinical paper on the use of ^{18}F in osteosarcoma is a case report by Tse et al. (*91*) on a patient with a history of congenital polyostotic fibrous dysplasia, metastatic osteogenic sarcoma, and a breast mass. This patient presented lung nodules with abnormal ^{18}F uptake, which was interpreted as diagnostic for osteosarcoma metastases.

Future Perspectives of ^{18}F

Thus, a wide field of research remains to be performed for ^{18}F in patients with osteosarcoma. Besides the unique potential of a more sensitive and specific tool than ^{18}F-FDG to detect metastases to the lungs or second bone sites for both

primary staging and restaging, ^{18}F may improve the sensitivity of conventional bone scanning in osteosarcoma patients: Schirrmeister et al. (*92–94*) found a higher sensitivity and accuracy of ^{18}F PET in detecting bone metastases in various cancers as compared with conventional bone scanning. Therefore, it seems promising to prospectively evaluate the clinical benefit of ^{18}F bone PET in comparison with bone scanning for the diagnostic work-up in osteosarcoma patients.

Monitoring the response to neoadjuvant chemotherapy with ^{18}F before surgical resection also seems to be a promising field of interest. This might allow detection of viable, nonnecrotic, and, thus, chemotherapy-resistant parts of the tumor as a possible predictor for therapy outcome and prognosis. Another focus of research might be to monitor the healing of bone grafts using ^{18}F to early detect local recurrences. Because ^{18}F is mainly incorporated in newly mineralized bone, whereas no uptake in inflammatory cells is to be expected, a differentiation of residual tumor or recurrence from postsurgical fibrotic changes, inflammation, or normal graft healing (Figs. 9 and 10) might be more reliable than by the use of ^{18}F-FDG. However, whether ^{18}F really can provide additional relevant information to imaging with FDG has to be investigated in further prospective patient studies.

CONCLUSION

In osteosarcoma the introduction of neoadjuvant chemotherapy has dramatically improved survival rates, changing the demands for state-of-the-art imaging to provide detailed information on tumor staging and grading, treatment evaluation, and detection of tumor recurrence. However, besides the studies published so far, it is not yet possible to draw definite conclusions resulting in approved indications for PET in osteosarcoma, mainly because of the small number of patients enrolled. Further research needs to be done in prospective studies in larger patient series to define the various indications that have been suggested as useful for osteosarcoma management. These indications are guiding biopsy in large heterogeneous primary tumors, predicting tumor response in neoadjuvant chemotherapy, differentiating postoperative changes from residual tumor tissue or local relapse, and whole-body imaging for detecting metastatic spread during follow-up.

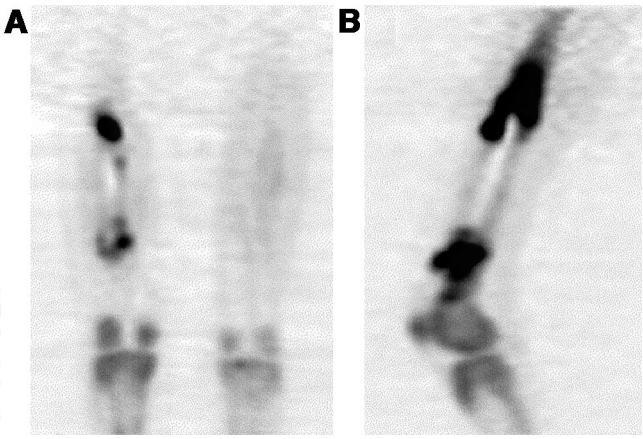

FIGURE 9. ^{18}F PET coronal (A) and sagittal (B) images in osteosarcoma patient 2 mo after surgery using full bone allograft. Intense tracer uptake at both ends of allograft (SUV, 21.0) characterizes active bone remodeling in early stage after surgery.

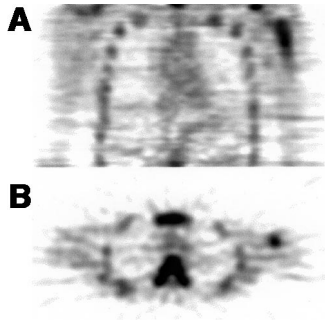

FIGURE 10. ^{18}F PET transverse (A) and coronal (B) images in osteosarcoma patient 23 mo after cancellous chip allografting of left proximal humerus. There is still tracer uptake, indicating increased bone formation. In comparison with Figure 9, however, tracer uptake is less, as shown by SUV of 4.8.

ACKNOWLEDGMENT

This work was supported in part by National Institutes of Health grant ROI CA 65537.

REFERENCES

1. Mirra JM. Osteosarcoma: intramedullary variants. In: Mirra JM, ed. *Bone Tumors.* Philadelphia, PA: Lea & Febiger; 1989:249–389.
2. American Joint Committee on Cancer. Bone. In: *AJCC Cancer Staging Manual.* 5th ed. Philadelphia, PA: Lippincott Raven; 1997:143–147.
3. Winkler K, Bieling P, Bielack S, et al. Local control and survival from the Cooperative Osteosarcoma Study Group studies of the German Society of Pediatric Oncology and the Vienna Bone Tumor Registry. *Clin Orthop.* 1991;270: 79–86.
4. Bruland OS, Pihl A. On the current management of osteosarcoma: a critical evaluation and a proposal for a modified treatment strategy. *Eur J Cancer.* 1997;33:1725–1731.
5. Arndt CA, Crist WM. Common musculoskeletal tumors of childhood and adolescence. *N Engl J Med.* 1999;341:342–352.
6. Resnick D, Greenway GD. Tumors and tumor-like lesions of bone: imaging and pathology of specific lesions. In: Resnick D, ed. *Bone and Joint Imaging.* Philadelphia, PA: Saunders; 1996:991–1063.
7. Sundaram M. The use of gadolinium in the MR imaging of bone tumors. *Semin Ultrasound CT MR.* 1997;18:307–311.
8. Seeger LL, Gold RH, Chandnani VP. Diagnostic imaging of osteosarcoma. *Clin Orthop.* 1991;270:254–263.
9. Dominkus M, Kainberger F, Lang S, Kotz R. Primary malignant bone tumors: clinical aspects and therapy—Vienna Bone Tumor Registry [in German]. *Radiologe.* 1998;38:472–482.
10. Fletcher BD. Imaging pediatric bone sarcomas: diagnosis and treatment-related issues. *Radiol Clin North Am.* 1997;35:1477–1494.
11. Focacci C, Lattanzi R, Iadeluca ML, Campioni P. Nuclear medicine in primary bone tumors. *Eur J Radiol.* 1998;27(suppl 1):S123–S131.
12. Davis AM, Bell RS, Goodwin PJ. Prognostic factors in osteosarcoma: a critical review. *J Clin Oncol.* 1994;12:423–431.
13. Kotz R, Ritschl P, Trachtenbrodt J. A modular femur-tibia reconstruction system. *Orthopedics.* 1986;9:1639–1652.
14. Kotz R, Salzer M. Rotation-plasty for childhood osteosarcoma of the distal part of the femur. *J Bone Joint Surg Am.* 1982;64:959–969.

15. Windhager R, Millesi H, Kotz R. Resection-replantation for primary malignant tumours of the arm: an alternative to fore-quarter amputation. *J Bone Joint Surg Br.* 1995;77:176–184.
16. Glasser DB, Lane JM, Huvos AG, Marcove RC, Rosen G. Survival, prognosis, and therapeutic response in osteogenic sarcoma: the Memorial Hospital experience. *Cancer.* 1992;69:698–708.
17. Picci P, Sangiorgi L, Rougraff BT, et al. Relationship of chemotherapy-induced necrosis and surgical margins to local recurrence in osteosarcoma. *J Clin Oncol.* 1994;12:2699–2705.
18. Bielack SS, Kempf-Bielack B, Delling G, et al. Prognostic factors in high-grade osteosarcoma of the extremities or trunk: an analysis of 1,702 patients treated on neoadjuvant cooperative osteosarcoma study group protocols. *J Clin Oncol.* 2002;20:776–790.
19. Saeter G, Hoie J, Stenwig AE, et al. Systemic relapse of patients with osteogenic sarcoma: prognostic factors for long term survival. *Cancer.* 1995;75:1084–1093.
20. Enneking WF, Spanier SS, Goodman MA. A system for the surgical staging of musculoskeletal sarcoma. *Clin Orthop.* 1980;153:106–120.
21. Enneking WF, Spanier SS, Goodman MA. Current concepts review: the surgical staging of musculoskeletal sarcoma. *J Bone Joint Surg Am.* 1980;62:1027–1030.
22. Kern KA, Brunetti A, Norton JA, et al. Metabolic imaging of human extremity musculoskeletal tumors by PET. *J Nucl Med.* 1988;29:181–186.
23. Adler LP, Blair HF, Makley JT, et al. Noninvasive grading of musculoskeletal tumors using PET. *J Nucl Med.* 1991;32:1508–1512.
24. Eary JF, O'Sullivan F, Powitan Y, et al. Sarcoma tumor FDG uptake measured by PET and patient outcome: a retrospective analysis. *Eur J Nucl Med.* 2002;29: 1149–1154.
25. Eary JF, Conrad EU. Positron emission tomography in grading soft tissue sarcomas. *Semin Musculoskelet Radiol.* 1999;3:135–138.
26. Eary JF, Conrad EU, Bruckner JD, et al. Quantitative [F-18]fluorodeoxyglucose positron emission tomography in pretreatment and grading of sarcoma. *Clin Cancer Res.* 1998;4:1215–1220.
27. Lodge MA, Lucas JD, Marsden PK, et al. A PET study of ^{18}FDG uptake in soft tissue masses. *Eur J Nucl Med.* 1999;26:22–30.
28. Nieweg OE, Pruim J, van Ginkel RJ, et al. Fluorine-18-fluorodeoxyglucose PET imaging of soft-tissue sarcoma. *J Nucl Med.* 1996;37:257–261.
29. Jones DN, McCowage GB, Sostman HD, et al. Monitoring of neoadjuvant therapy response of soft-tissue and musculoskeletal sarcoma using fluorine-18-FDG PET. *J Nucl Med.* 1996;37:1438–1444.
30. Schulte M, Brecht-Krauss D, Werner M, et al. Evaluation of neoadjuvant therapy response of osteogenic sarcoma using FDG PET. *J Nucl Med.* 1999;40:1637–1643.
31. Stokkel MP, Draisma A, Pauwels EK. Positron emission tomography with 2-[^{18}F]-fluoro-2-deoxy-D-glucose in oncology. Part IIIb. Therapy response monitoring in colorectal and lung tumours, head and neck cancer, hepatocellular carcinoma and sarcoma. *J Cancer Res Clin Oncol.* 2001;127:278–285.
32. Franzius C, Sciuk J, Brinkschmidt C, Jurgens H, Schober O. Evaluation of chemotherapy response in primary bone tumors with F-18 FDG positron emission tomography compared with histologically assessed tumor necrosis. *Clin Nucl Med.* 2000;25:874–881.
33. Garcia R, Kim EE, Wong FC, et al. Comparison of fluorine-18-FDG PET and technetium-99m-MIBI SPECT in evaluation of musculoskeletal sarcomas. *J Nucl Med.* 1996;37:1476–1479.
34. Hicks RJ. Nuclear medicine techniques provide unique physiologic characterization of suspected and known soft tissue and bone sarcomas. *Acta Orthop Scand Suppl.* 1997;273:25–36.
35. Kole AC, Nieweg OE, van Ginkel RJ, et al. Detection of local recurrence of soft-tissue sarcoma with positron emission tomography using [^{18}F]fluorodeoxyglucose. *Ann Surg Oncol.* 1997;4:57–63.
36. Lucas JD, O'Doherty MJ, Wong JC, et al. Evaluation of fluorodeoxyglucose positron emission tomography in the management of soft-tissue sarcomas. *J Bone Joint Surg Br.* 1998;80:441–447.
37. Page RL, Garg PK, Garg S, et al. PET imaging of osteosarcoma in dogs using a fluorine-18-labeled monoclonal antibody Fab fragment. *J Nucl Med.* 1994;35: 1506–1513.
38. Rasey JS, Koh WJ, Grierson JR, Grunbaum Z, Krohn KA. Radiolabelled fluoromisonidazole as an imaging agent for tumor hypoxia. *Int J Radiat Oncol Biol Phys.* 1989;17:985–991.
39. Haubner R, Wester HJ, Burkhart F, et al. Glycosylated RGD-containing peptides: tracer for tumor targeting and angiogenesis imaging with improved biokinetics. *J Nucl Med.* 2001;42:326–336.
40. Haubner R, Wester HJ, Weber WA, et al. Noninvasive imaging of alpha(v)beta3 integrin expression using ^{18}F- labeled RGD-containing glycopeptide and positron emission tomography. *Cancer Res.* 2001;61:1781–1785.
41. Sordillo PP, Benua RS, Gelbard AS, et al. Imaging of human tumors and organs with N-13-labeled L-methionine. *Am J Physiol Imaging.* 1986;1:195–200.
42. Doubrovin M, Ponomarev V, Beresten T, et al. Imaging transcriptional regulation of p53-dependent genes with positron emission tomography in vivo. *Proc Natl Acad Sci USA.* 2001;98:9300–9305.
43. Ichiya Y, Kuwabara Y, Otsuka M, et al. Assessment of response to cancer therapy using fluorine-18-fluorodeoxyglucose and positron emission tomography. *J Nucl Med.* 1991;32:1655–1660.
44. Patlak CS, Blasberg RG. Graphical evaluation of blood-to-brain transfer constants from multiple-time uptake data: generalizations. *J Cereb Blood Flow Metab.* 1985;5:584–590.
45. Patlak CS, Blasberg RG, Fenstermacher JD. Graphical evaluation of blood-to-brain transfer constants from multiple-time uptake data. *J Cereb Blood Flow Metab.* 1983;3:1–7.
46. Gjedde A. Calculation of cerebral glucose phosphorylation from brain uptake of glucose analogs in vivo: a re-examination. *Brain Res.* 1982;257:237–274.
47. Phelps ME, Huang SC, Hoffman EJ, et al. Tomographic measurement of local cerebral glucose metabolic rate in humans with (F-18)2-fluoro-2-deoxy-D-glucose: validation of method. *Ann Neurol.* 1979;6:371–388.
48. Hoh CK, Hawkins RA, Glaspy JA, et al. Cancer detection with whole-body PET using 2-[^{18}F]fluoro-2-deoxy-D-glucose. *J Comput Assist Tomogr.* 1993;17:582–589.
49. Kole AC, Nieweg OE, Hoekstra HJ, et al. Fluorine-18-fluorodeoxyglucose assessment of glucose metabolism in bone tumors. *J Nucl Med.* 1998;39:810–815.
50. Griffeth LK, Dehdashti F, McGuire AH, et al. PET evaluation of soft-tissue masses with fluorine-18 fluoro-2-deoxy-D-glucose. *Radiology.* 1992;182:185–194.
51. Dehdashti F, Siegel BA, Griffeth LK, et al. Benign versus malignant intraosseous lesions: discrimination by means of PET with 2-[F-18]fluoro-2-deoxy-D-glucose. *Radiology.* 1996;200:243–247.
52. Eary JF, Mankoff DA. Tumor metabolic rates in sarcoma using FDG PET. *J Nucl Med.* 1998;39:250–254.
53. Folpe AL, Lyles RH, Sprouse JT, Conrad EU 3rd, Eary JF. (F-18) fluorodeoxyglucose positron emission tomography as a predictor of pathologic grade and other prognostic variables in bone and soft tissue sarcoma. *Clin Cancer Res.* 2000;6:1279–1287.
54. Schulte M, Brecht-Krauss D, Heymer B, et al. Grading of tumors and tumorlike lesions of bone: evaluation by FDG PET. *J Nucl Med.* 2000;41:1695–1701.
55. Aoki J, Watanabe H, Shinozaki T, et al. FDG PET of primary benign and malignant bone tumors: standardized uptake value in 52 lesions. *Radiology.* 2001;219:774–777.
56. Watanabe H, Shinozaki T, Yanagawa T, et al. Glucose metabolic analysis of musculoskeletal tumours using 18fluorine-FDG PET as an aid to preoperative planning. *J Bone Joint Surg Br.* 2000;82:760–767.
57. Franzius C, Bielack S, Flege S, et al. Prognostic significance of ^{18}F-FDG and ^{99m}Tc-methylene diphosphonate uptake in primary osteosarcoma. *J Nucl Med.* 2002;43:1012–1017.
58. Messa C, Landoni C, Pozzato C, Fazio F. Is there a role for FDG PET in the diagnosis of musculoskeletal neoplasms [commentary]? *J Nucl Med.* 2000;41: 1702–1703.
59. Wuisman P, Enneking WF. Prognosis for patients who have osteosarcoma with skip metastasis. *J Bone Joint Surg Am.* 1990;72:60–68.
60. Fletcher BD, Hanna SL. Pediatric musculoskeletal lesions simulating neoplasms. *Magn Reson Imaging Clin N Am.* 1996;4:721–747.
61. Bhagia SM, Grimer RJ, Davies AM, Mangham DC. Scintigraphically negative skip metastasis in osteosarcoma. *Eur Radiol.* 1997;7:1446–1448.
62. Franzius C, Daldrup-Link HE, Sciuk J, et al. FDG-PET for detection of pulmonary metastases from malignant primary bone tumors: comparison with spiral CT. *Ann Oncol.* 2001;12:479–486.
63. Franzius C, Daldrup-Link HE, Wagner-Bohn A, et al. FDG-PET for detection of recurrences from malignant primary bone tumors: comparison with conventional imaging. *Ann Oncol.* 2002;13:157–160.
64. Franzius C, Sciuk J, Daldrup-Link HE, Jurgens H, Schober O. FDG-PET for detection of osseous metastases from malignant primary bone tumours: comparison with bone scintigraphy. *Eur J Nucl Med.* 2000;27:1305–1311.
65. Daldrup-Link HE, Franzius C, Link TM, et al. Whole-body MR imaging for detection of bone metastases in children and young adults: comparison with skeletal scintigraphy and FDG PET. *AJR.* 2001;177:229–236.
66. Lawrence JA, Babyn PS, Chan HS, et al. Extremity osteosarcoma in childhood: prognostic value of radiologic imaging. *Radiology.* 1993;189:43–47.
67. Nair N, Ali A, Green AA, et al. Response of osteosarcoma to chemotherapy: evaluation with F-18 FDG-PET scans. *Clin Positron Imaging.* 2000;3:79–83.
68. Hawkins DS, Rajendran JG, Conrad EU 3rd, Bruckner JD, Eary JF. Evaluation

of chemotherapy response in pediatric bone sarcomas by [F-18]-fluorodeoxy-D-glucose positron emission tomography. *Cancer.* 2002;94:3277–3284.
69. Abdel-Dayem HM. The role of nuclear medicine in primary bone and soft tissue tumors. *Semin Nucl Med.* 1997;27:355–363.
70. Fletcher BD. Response of osteosarcoma and Ewing sarcoma to chemotherapy: imaging evaluation. *AJR.* 1991;157:825–833.
71. Ma LD, Frassica FJ, Scott WW Jr, Fishman EK, Zerbouni EA. Differentiation of benign and malignant musculoskeletal tumors: potential pitfalls with MR imaging. *Radiographics.* 1995;15:349–366.
72. Lang P, Wendland MF, Saeed M, et al. Osteogenic sarcoma: noninvasive in vivo assessment of tumor necrosis with diffusion-weighted MR imaging. *Radiology.* 1998;206:227–235.
73. Reddick WE, Bhargava R, Taylor JS, Meyer WH, Fletcher BD. Dynamic contrast-enhanced MR imaging evaluation of osteosarcoma response to neoadjuvant chemotherapy. *J Magn Reson Imaging.* 1995;5:689–694.
74. Reddick WE, Wang S, Xiong X, et al. Dynamic magnetic resonance imaging of regional contrast access as an additional prognostic factor in pediatric osteosarcoma. *Cancer.* 2001;91:2230–2237.
75. el-Zeftawy H, Heiba SI, Jana S, et al. Role of repeated F-18 fluorodeoxyglucose imaging in management of patients with bone and soft tissue sarcoma. *Cancer Biother Radiopharm.* 2001;16:37–46.
76. Baldini N, Scotlandi K, Barbanti-Brodano G, et al. Expression of P-glycoprotein in high-grade osteosarcomas in relation to clinical outcome. *N Engl J Med.* 1995;333:1380–1385.
77. Baldini N, Scotlandi K, Serra M, et al. P-glycoprotein expression in osteosarcoma: a basis for risk-adapted adjuvant chemotherapy. *J Orthop Res.* 1999;17:629–632.
78. Serra M, Maurici D, Scotlandi K, et al. Relationship between P-glycoprotein expression and p53 status in high-grade osteosarcoma. *Int J Oncol.* 1999;14:301–307.
79. Green JR, Reeve J, Tellez M, Veall N, Wootton R. Skeletal blood flow in metabolic disorders of the skeleton. *Bone.* 1987;8:293–297.
80. Wootton R, Dore C. The single-passage extraction of ^{18}F in rabbit bone. *Clin Phys Physiol Meas.* 1986;7:333–343.
81. Garnett ES, Bowen BM, Coates G, Nahmias C. An analysis of factors which influence the local accumulation of bone-seeking radiopharmaceuticals. *Invest Radiol.* 1975;10:564–568.
82. Nahmias C, Cockshott WP, Belbeck LW, Garnett ES. Measurement of absolute bone blood flow by positron emission tomography. *Skeletal Radiol.* 1986;15:198–200.
83. Hawkins RA, Choi Y, Huang SC, et al. Evaluation of the skeletal kinetics of fluorine-18-fluoride ion with PET. *J Nucl Med.* 1992;33:633–642.
84. Grynpas MD. Fluoride effects on bone crystals. *J Bone Miner Res.* 1990;5(suppl 1):S169–S175.
85. Cook GJ, Lodge MA, Marsden PK, Dynes A, Fogelman I. Non-invasive assessment of skeletal kinetics using fluorine-18 fluoride positron emission tomography: evaluation of image and population-derived arterial input functions. *Eur J Nucl Med.* 1999;26:1424–1429.
86. Piert M, Machulla HJ, Jahn M, et al. Coupling of porcine bone blood flow and metabolism in high-turnover bone disease measured by [^{15}O]H_2O and [^{18}F]fluoride ion positron emission tomography. *Eur J Nucl Med Mol Imaging.* 2002;29:907–914.
87. Piert M, Winter E, Becker GA, et al. Allogenic bone graft viability after hip revision arthroplasty assessed by dynamic [^{18}F]fluoride ion positron emission tomography. *Eur J Nucl Med.* 1999;26:615–624.
88. Piert M, Zittel TT, Becker GA, et al. Assessment of porcine bone metabolism by dynamic [^{18}F]fluoride ion PET: correlation with bone histomorphometry. *J Nucl Med.* 2001;42:1091–1100.
89. Blau M, Nagler W, Bender MA. A new isotope for bone scanning. *J Nucl Med.* 1962;3:332–334.
90. Hoh CK, Hawkins RA, Dahlbom M, et al. Whole body skeletal imaging with [^{18}F]fluoride ion and PET. *J Comput Assist Tomogr.* 1993;17:34–41.
91. Tse N, Hoh C, Hawkins R, Phelps M, Glaspy J. Positron emission tomography diagnosis of pulmonary metastases in osteogenic sarcoma. *Am J Clin Oncol.* 1994;17:22–25.
92. Schirrmeister H, Glatting G, Hetzel J, et al. Prospective evaluation of the clinical value of planar bone scans, SPECT, and ^{18}F-labeled NaF PET in newly diagnosed lung cancer. *J Nucl Med.* 2001;42:1800–1804.
93. Schirrmeister H, Guhlmann A, Elsner K, et al. Sensitivity in detecting osseous lesions depends on anatomic localization: planar bone scintigraphy versus ^{18}F PET. *J Nucl Med.* 1999;40:1623–1629.
94. Schirrmeister H, Guhlmann A, Kotzerke J, et al. Early detection and accurate description of extent of metastatic bone disease in breast cancer with fluoride ion and positron emission tomography. *J Clin Oncol.* 1999;17:2381–2389.

JNM The Journal of NUCLEAR MEDICINE

PET Imaging of Osteosarcoma

Winfried Brenner, Karl H. Bohuslavizki and Janet F. Eary

J Nucl Med. 2003;44:930-942.

The Journal of Nuclear Medicine is published monthly.
SNMMI | Society of Nuclear Medicine and Molecular Imaging
1850 Samuel Morse Drive, Reston, VA 20190.
(Print ISSN: 0161-5505, Online ISSN: 2159-662X)

SNMMI SOCIETY OF NUCLEAR MEDICINE AND MOLECULAR IMAGING